JOURNAL OF APPLIED ELECTROCHEMISTRY **28** (1998) 461–469

SHORT COMMUNICATION

Electrodeposition of copper on thermally oxidized 316 L stainless steel substrates

Z. ZHOU, T. J. O'KEEFE
Department of Metallurgical Engineering and Graduate Center for Materials Research, University of Missouri-Rolla, Rolla, Missouri 65409-1170, USA

Received 12 November 1996; revised 10 April 1997

The effect of thermal oxidation of 316 L stainless steel cathode blanks used in copper electrodeposition was studied. Current and potential step experiments were performed to evaluate electrochemical changes caused by the oxidation treatments. SEM and AES were used to characterize the stainless steel substrates and the deposited copper films. Particular emphasis was given to the initial stages of copper nucleation and growth. The copper electrocrystallization process was strongly influenced by the temperature employed in oxidizing the stainless steel. Dense, uniform and fine copper nuclei were obtained on the stainless steel substrate oxidized in air at 200 °C and 300 °C for 3 h. The copper nucleation density and uniformity decreased considerably on substrates treated at 500 °C and 600 °C. Attempts were made to identify changes in the mechanism of copper nucleation on the various oxidized stainless steel substrates using models developed by Thirsk and Harrison.

Keywords: *copper deposition*, *electrocrystallization*, *thermally treated stainless steel*

1. Introduction

Stainless steel and titanium are both commonly used as cathode blanks in copper electrowinning. Currently, stainless steel is preferred, but titanium does offer an alternative in selected cases. Cathode blanks usually give a purer copper product and more efficient materials handling compared to operations employing starter sheets.

Several studies focused on the electrodeposition of copper on cathodes with different surface pretreatments, such as anodizing, mechanical and chemical polishing [1–3]. Rao and Cooper [4, 5] studied the nucleation and growth behaviour of the copper electrodeposits on substrates such as emulsion-coated copper, copper covered with benzothiazolethiol (BTAT), black anodized titanium, conditioned titanium and cold rolled vacuum annealed titanium. The BTAT-coated copper gave a dense uniform deposit free from laciness. Conversely, the deposits on the copper with the emulsion film, on the conditioned titanium and on black anodized titanium, were non-uniform. The size of the crystals deposited on these substrates was larger than those on the BTAT-coated surface. Growth was likely angular with a few dendrites grown on the emulsion-coated copper substrates.

A study of electrodeposits of copper onto highly perfect electropolished (0 0 1) faces of copper single crystals was made by Cusminsky [6]. As-grown, annealed and deformed single crystals were used. It was found that the growth on annealed single crystals changes from single crystalline to polycrystalline at higher thicknesses than on the other substrates at all current densities from 10–80 mA cm^{-2} in his study. Recently, Zhang [7] and Teng [8] studied the electrodeposition of copper on plasma and thermally oxidized titanium substrates. It was found that the nucleation and growth of copper electrodeposited on titanium substrates varied substantially for the different treatments and the mechanisms controlling the copper nucleation and growth were examined and correlated with the initial surface oxide. Thus, there was some evidence that prior surface treatment could modify the nature of performance of copper deposition, particularly on oxidized surfaces.

In this study, 316 L stainless steel substrates were thermally oxidized at various temperatures ranging from 200 °C to 600 °C. AES and SEM techniques were used to characterize the thin films produced. The electrochemical behaviour of the various oxides with respect to the polarization and the nucleation of copper electrodeposited on the pretreated stainless steel was then investigated. Where possible, the mechanisms controlling the initial deposition behaviour were determined.

2. Experimental details

2.1. *Thermal oxidation*

Stainless steel electrodes (6 cm × 1.4 cm) were made from 316 L stainless steel sheets about 1 mm thick. The working electrodes were prepared by wet grinding on 600 grit paper and cleaning with acetone in an ultrasonic bath for 5 min. The oxidation treatments were conducted in air at ambient pressure for 3 h in

the temperature range from 200 to 600 °C. A number of samples were made and the reproducibility was quite good, particularly with regard to the trends.

2.2. *Deposition system*

A copper sulfate–sulfuric acid electrolyte was used for the deposition studies. The solutions were prepared from Fisher certified grade cupric sulfate pentahydrate and reagent grade sulfuric acid to give a stock electrolyte concentration of $40\,g\,dm^{-3}$ copper and $180\,g\,dm^{-3}$ sulfuric acid. The temperature of the electrolyte was maintained at 40 °C for all of the electrochemical tests.

Platinum was the counter electrode and a mercury/mercurous sulfate electrode (+656 mV vs SHE) was used as the reference. All potentials are reported with respect to the mercury/mercurous sulfate reference electrode.

2.3. *Electrochemical tests*

2.3.1. Potentiodynamic measurements. A EG&G Parc model 273 potentiostat/galvanostat was used for the cyclic voltammetry measurements. The voltammograms were started at −350 mV vs Hg/Hg_2SO_4 and then driven in the cathodic direction to −700 mV before reversing to the initial potential, all at a scan rate of $10\,mV\,s^{-1}$.

2.3.2. Potential step measurements. A cathodic potential of −600 mV vs Hg/Hg_2SO_4 was applied to the pretreated stainless steel cathodes for the potential step experiments. The values of the current densities were obtained as a function of time and stored for analysis of the nucleation mechanism. The curves for the current densities against $(t - t_0)^n$ were plotted, where t_0 is the initial time at which the current flow is minimum and n is related to the particular nucleation mechanism, as described by Thirsk and Harrison [9].

2.3.3. Current step measurements. A EG&G Parc model 273 potentiostat/galvanostat was also used to generate the current step data. Deposits of 10 s were made galvanostatically at a current density of $3\,mA\,cm^{-2}$ on the various stainless steel electrodes. The resulting copper deposits were then prepared for SEM evaluation.

2.4. *Resistance measurements*

Resistance was measured by using a four point probe (Alessi Co.) in conjunction with a Keithley model 181 nanovoltmeter and model 220 programmable current source.

2.5. *SEM and AES examination*

A Jeol T330A scanning electron microscope was used to examine the copper deposited on the various stainless steel substrates. Surface composition profile analyses of treated stainless steel substrates were carried out with a Physical Electronics model 545 Auger electron spectrometer operated at an initial pressure below 5×10^{-9} torr. The depth composition profiling of the treated stainless steel substrates was obtained by argon ion sputtering at a pressure of 5×10^{-5} torr with a voltage of 2 kV and a current of 10 mA. The approximate sputter rate was $15\,Å\,min^{-1}$.

3. Results and discussion

3.1. *Oxidation treatments*

The oxide colour, thickness and conductivity changed with oxidation temperature, as shown in Table 1. As the treatment temperature increased from 200 to 600 °C, the colour changed from light gold to dark gold and finally blue. A similar relationship between thickness and colour has been reported for oxidized titanium [10].

Table 1 also shows the resistance change of the stainless steel with different surface treatments. Generally, the resistance increased with the temperature of treatment, with values ranging from 9.5 to 25.7 mΩ.

Auger surface composition profile analyses were performed on the stainless steel with and without oxidation treatment and presented as the weight percentage of the principal elements versus sputtering depth. For each profile, the elements Cr, Fe, O, C, Ni and Mo were monitored. The Auger peaks were computer differentiated and the peak-to-peak height values for each element were normalized to a common reference, as recommended by the manufacturer.

Carbon contamination was rapidly removed and reached a constant value after a few minutes of sputtering for each sample. Since C, Ni and Mo gave similar curves and compositions regardless of treat-

Table 1. Colour, oxide thickness and conductivity of stainless steel substrates with different surface treatments

Temperature/°C	*Treat time*/h	*Thickness*/Å	*Colours*	10^{-3} *Resistance*/Ω
untreated (600-grit polishing)		45	colourless	9.5
as-received		140	colourless	9.5
200	3 (air)	240	light gold	10.3
300	3 (air)	250	gold	10.4
400	3 (air)	260	dark gold	10.5
500	3 (air)	360	copper	12.6
600	3 (air)	540	blue	25.7

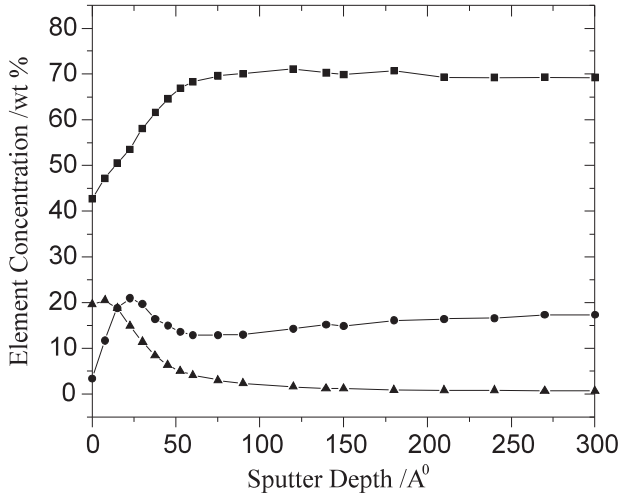

Fig. 1. Auger compositional depth profile of 316 L stainless steel without furnace treatment (600 grit polishing). Key: (■) Fe; (●) Cr; (▲) O.

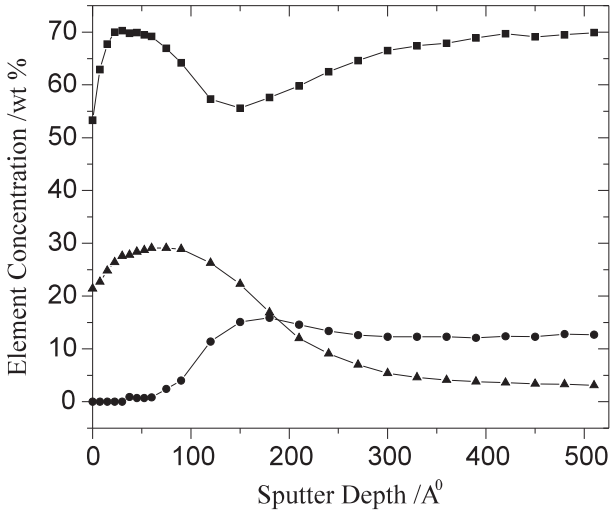

Fig. 3. Auger compositional depth profile of 316 L stainless steel with 3 h furnace treatment at 200 °C. Key: (■) Fe; (●) Cr; (▲) O.

ment, only the three main elements Fe, Cr and O are shown.

The Auger results are shown in Figs 1–5. A similar trend for Cr composition was obtained on the samples with or without treatment. The relative chromium concentration was low at the surface and went through a peak concentration before gradually decreasing to a constant concentration into the bulk alloy. The thickness value where a peak occurred changed with treatment temperature. For the stainless steel without furnace treatment shown in Fig. 1 (600-grit polishing) and Fig. 2 (as-received), a narrow peak located at 25 Å and 90 Å was found. For the stainless steel oxidized at 200, 400 and 500 °C (Figs 3, 4 and 5), the Cr peak concentration was higher and was located deeper into the surface. The positions where the maxima occurred were approximately at 170, 190 and 210 Å and this trend became more obvious with increasing oxidization temperature.

Two trends were observed for the variation of iron concentration with depth. For the unoxidized samples (Figs 1 and 2), the relative iron concentration was low at the surface and gradually increased with thickness until a constant concentration was reached. For oxidized samples, the relative iron concentration was lower at the surface and went through a peak concentration, before gradually increasing to the constant concentration of the alloy. The peak became broader and the minimum concentration was lower as the oxidizing temperature was increased from 200 to 500 °C, as shown in Figs 3, 4 and 5.

According to the Auger electron spectrometer (AES) analyses, the oxide film thickness increased with temperature as did the relative Cr and Fe concentrations shown in Figs 1–5. These data are assumed to be semiquantitative in nature and used to show trends rather than precise oxide compositions. For untreated samples, the oxide was relatively thin, being 45 Å for 600-grit polished sample and 140 Å for as-received sample. The oxygen concentration near the surface of the untreated samples was relatively low, being approximately 20 wt %. For the stainless

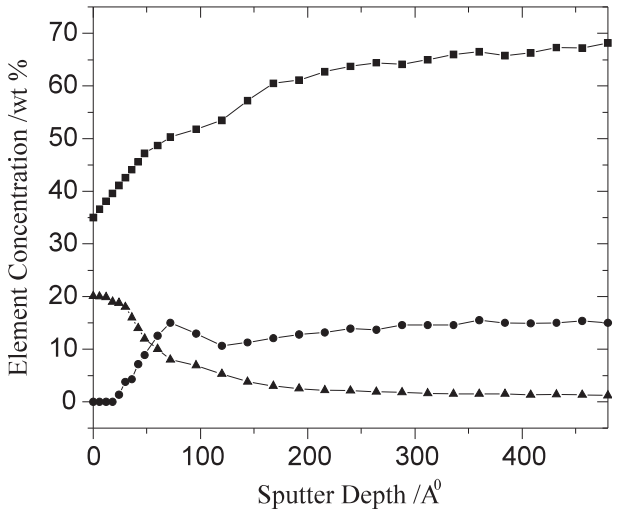

Fig. 2. Auger compositional depth profile of 316 L stainless steel without furnace treatment (as-received). Key: (■) Fe; (●) Cr; (▲) O.

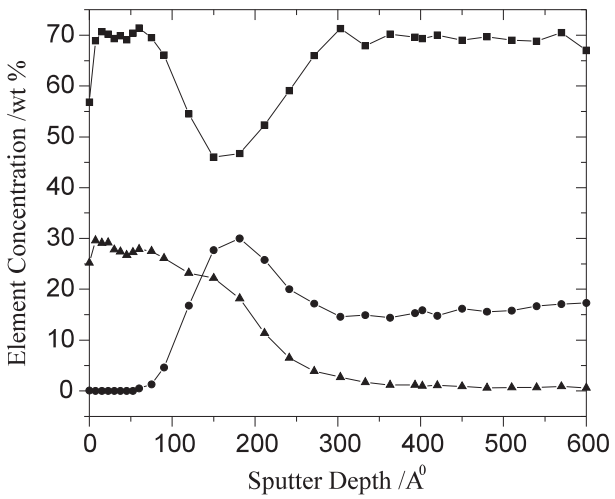

Fig. 4. Auger compositional depth profile of 316 L stainless steel with 3 h furnace treatment at 400 °C. Key: (■) Fe; (●) Cr; (▲) O.

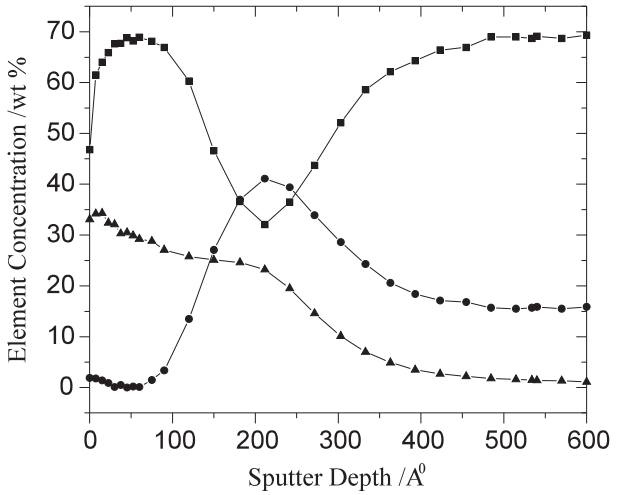

Fig. 5. Auger compositional depth profile of 316 L stainless steel with 3 h furnace treatment at 500 °C. Key: (■) Fe; (●) Cr; (▲) O.

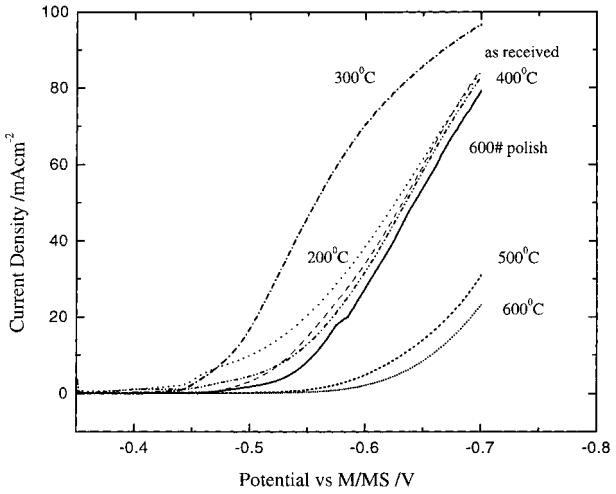

Fig. 6. Polarization curves obtained from a copper electrolyte (40 g dm^{-3} Cu^{2+}, 180 g dm^{-3} H_2SO_4) using stainless steel substances as-received, polished and pretreated for 3 h at different furnace temperatures. Key: (———) 600 grit polish; (– – – –) as-received; (· · · · ·) 200 °C; (–·–·–) 300 °C; (–··–··–) 400 °C; (·····) 500 °C; (——) 600 °C.

sample oxidized at 200 °C, the peak with a value of about 30 wt % near the outer surface was obtained and the thickness of oxide was about 240 Å. The stainless steel sample treated at 500 °C had a broader oxygen composition profile also near 30 wt %, but the thickness was 360 Å.

The iron, chromium and oxygen ratios appear to be important with respect to influencing initial copper nucleation. Subsequent results show that copper nucleation was suppressed on the stainless steel substrates treated at temperatures above 400 °C, but was enhanced on the substrates treated at 200 °C and 300 °C when compared with the untreated sample (600-grit polishing).

3.2. *Polarization measurements*

The influence of oxidizing the stainless steel substrates on the polarization curves in an acidic copper sulfate electrolyte can be observed in Fig. 6. For the stainless steel substrates furnace oxidized at or above 500 °C, the overpotential for copper nucleation became more negative or polarized and nucleation and growth were suppressed, compared with an untreated stainless steel electrode (600-grit polishing). The polarization tendency further increased as the treatment temperature increased from 500 to 600 °C possibly because of the higher resistivity and a higher Cr/Fe ratio. The increase in polarization values were approximately 80 mV and 100 mV, respectively. The values measured could be expected to vary as much as 5 mV. The stainless steel substrate polished with 600-grit also polarized the electrode reaction, but the value was only about 20 mV when compared with an untreated stainless steel electrode.

As seen in Fig. 6, for the stainless steel substrates oxidized below 400 °C the overpotential for copper nucleation became more positive or depolarized and nucleation and growth were enhanced, compared with an untreated sample. The values were approximately 30 mV at 400 °C and 45 mV at 300 °C and 200 °C, but the curve for the 300 °C surface became somewhat polarized after the initial stages of nucleation.

3.3. *SEM examination*

3.3.1. Potential step measurements. The morphology and surface coverage of copper nucleated at −600 mV vs Hg/Hg_2SO_4 on the oxidized stainless steel substrates were examined using SEM techniques. The deposition time was 0.5 s except for the highly polarized surfaces oxidized at 500 °C and 600 °C where 1.5 s was needed to get a suitable deposit.

The SEM micrographs of copper nucleated on the 600-grit polished stainless steel substrates are shown in Fig. 7(a). A low density of small copper nuclei was found after 0.5 s deposition which were relatively fine and uniform in size (0.1 to 1 μm) with some aggregation in evidence. For the stainless steel substrate oxidized at 200 °C, the copper nucleation was very dense after 0.5 s deposition particularly along the polishing marks (Fig. 7(b)). The copper nuclei appeared to be very uniform in size, indicating the mechanism for this substrate is probably instantaneous nucleation but some particle aggregation was noted. A similar pattern of copper nucleation was formed on the as-received stainless steel except the density was low, but evenly distributed (Fig. 7(c)). When the temperature was increased to 300 °C, the surface was covered with slightly larger copper crystals but with less uniformity (Fig. 7(d)) compared with the 200 °C treated stainless steel substrate. At the lower treatment temperatures, copper nucleation was enhanced with a high degree of electrode coverage and relatively uniform nuclei size.

For the stainless steel substrate treated at 500 °C (Fig. 7(e)), a very low density of larger and nonuniform copper nuclei (up to a few micrometre) were obtained after 1.5 s deposition. As the treatment temperature increased to 600 °C (Fig. 7(f)), copper

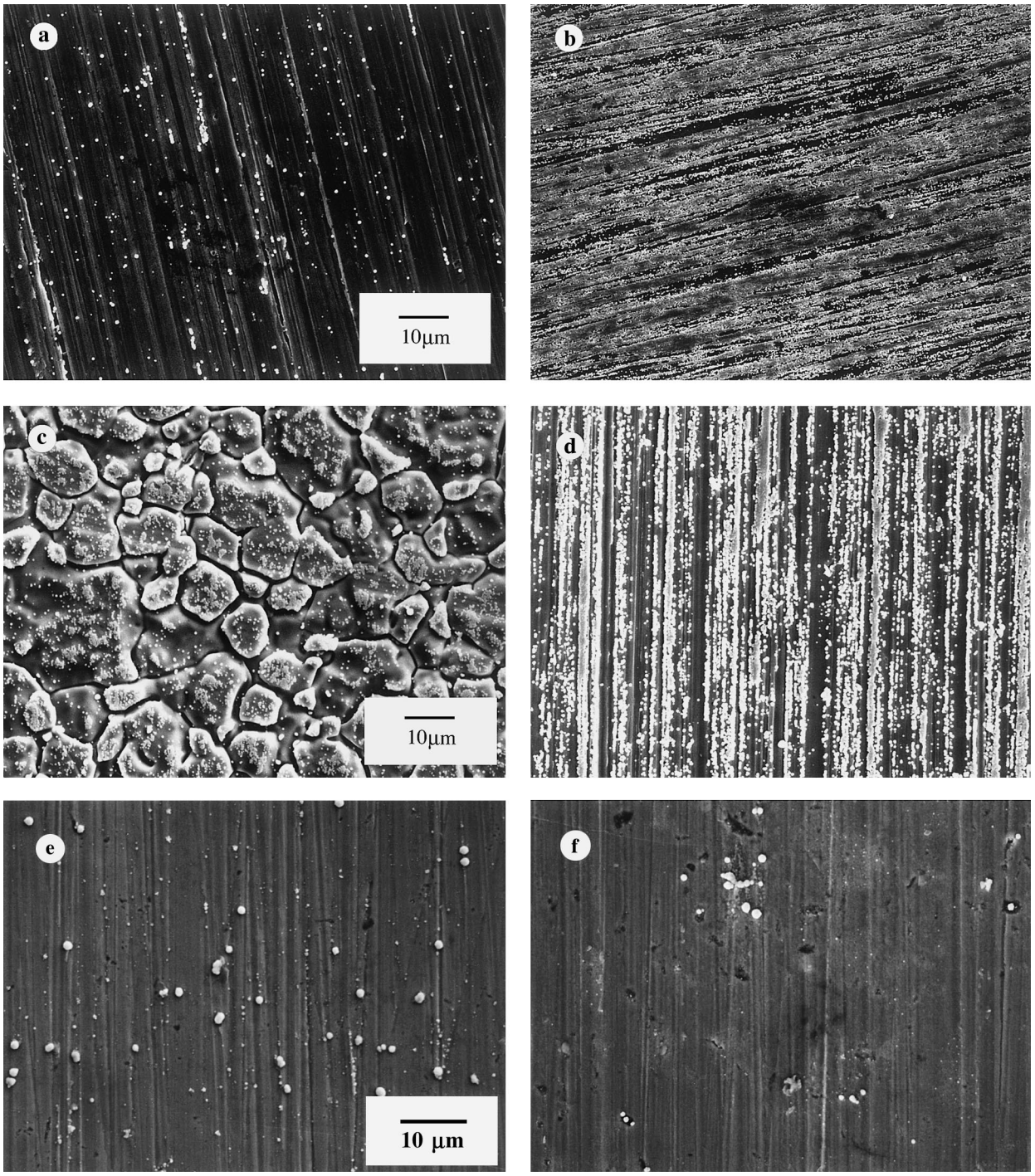

Fig. 7. Copper deposited at −600 mV vs Hg/Hg_2SO_4 on different stainless steel substrates; (a) 600 grit polishing, 0.5 s; (b) 200 °C furnace treatment, 0.5 s deposit 1000×; (c) as received for 0.5 s; (d) 300 °C furnace treatment for 0.5 s deposit; (e) 500 °C furnace treatment, 1.5 s; (f) 600 °C furnace treatment, 1.5 s deposit.

nuclei formed, but with the least density of all the surfaces evaluated. The unequal size distribution of the copper crystals indicated the nucleation was progressive for the 500 °C and 600 °C furnace treated stainless steel.

The results of the SEM examination implied that the 316 L stainless steel oxide film formed at higher temperatures acted as a blocking film and limited favorable sites for the copper nucleation, whereas the stainless steel oxide films formed during lower temperature oxidation promoted high density nucleation.

3.3.2. Current step measurements. The SEM micrographs of copper nucleated on the various stainless steel substrates using a current step technique are shown in Fig. 8. The current density was 3 mA cm^{-2} and deposition time was 10 s. Trends similar to those using the potential step technique were obtained. For 600 grit polished stainless steel (Fig. 8(a)), the copper nuclei appeared to be relatively fine (up to 2 μm) but with low coverage. A high density of fine copper nuclei were formed on the 200 °C oxidized stainless steel (Fig. 8(b)). The nuclei were relatively uniform (up to 1 μm) and preferred nucleation occurred

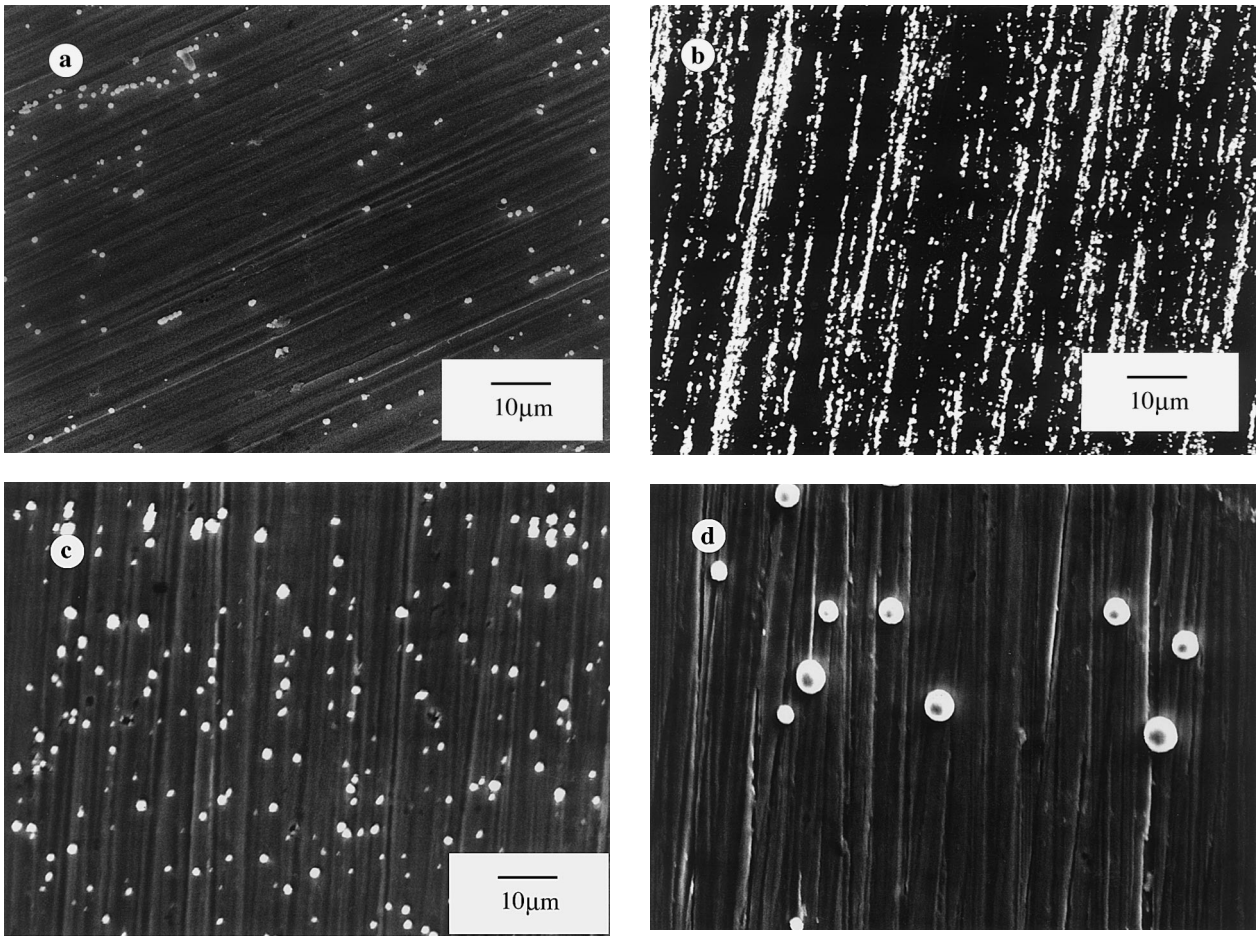

Fig. 8. Copper deposited with c.d. 3 mA cm^{-2} on different stainless steel substrates: (a) 600 grit polishing, 10 s deposit; (b) 200 °C furnace treatment, 10 s deposit; (c) 500 °C furnace treatment, 10 s deposit; (d) 600 °C furnace treatment, 10 s deposit. Magnification 1000×.

along the polishing marks. At the higher treatment temperatures, copper nucleation was suppressed with a lower degree of coverage and larger nuclei size being observed. The size distribution was relatively nonuniform. Figures 8(c) and 8(d) show the results obtained using 500 °C and 600 °C oxidized stainless steels as cathodes. The nuclei size was much larger and increased from about 3 to 6 μm when the temperature increased from 500 to 600 °C.

The morphology studies suggest that copper nucleation and growth on the oxidized stainless substrates was strongly influenced by the nature of oxide surface. In particular, changes in the nuclei density and size, morphology, coverage and probably the nucleation mechanism of the copper deposits were observed.

3.4. *Potential step measurements*

In general, three characteristic regions can be observed in the current-time deposition curves. These included an initial short time high current density pulse which was related to the double layer charging transient. An incubation period of low and essentially constant current then occurred which was followed by the nucleation and growth process. In some cases, the incubation time may be too short to be observed on the plots. Figure 9 shows the current–time curves for copper electrodeposition on the oxidized stainless steel substrates using the acid copper sulfate electrolyte (40 g dm^{-3} Cu, 180 g dm^{-3} H_2SO_4). The initial pulse of the current–time curves is not shown because the various surface treatment conditions had almost

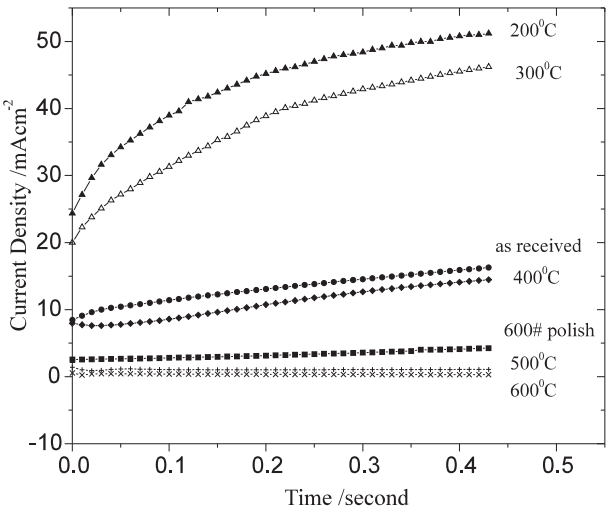

Fig. 9. Current–time transients for the deposition of copper on various furnace treated stainless steels from a copper sulfate electrolyte (40 g dm^{-3} Cu^{2+}, 180 g dm^{-3} H_2SO_4) 40 °C and −600 mV vs Hg/Hg_2SO_4. Key: (–■–) 600 grit polish; (–●–) as-received; (–◆–) 400 °C; (–▲–) 200 °C; (–+–) 500 °C; (–×–) 600 °C; (–△–) 300 °C.

no effect on their intensity or duration. Based on the observed results, the current response of the furnace oxidized stainless steel electrodes during copper electrodeposition can also be separated into two categories when compared with the untreated sample (600-grit polishing). For the electrodes treated at the temperature lower than 400 °C, the apparent current density for copper nucleation and growth is higher than that of the untreated electrode. As the treatment temperature decreased, the corresponding current density for deposition increased. For the electrodes treated above 400 °C, the current density was lower than for untreated electrodes (600-grit polishing) and the incubation time was longer as temperature increased. For the surfaces treated at 500 °C and 600 °C no current flow was shown indicating that an incubation time may exist whose duration is in excess of 0.5 s. Longer test times would be required to substantiate these observations. These trends were in agreement with the results obtained from the polarization curve measurements.

The potential step data were used to analyse the mechanism of copper nucleation. According to Thirsk and Harrison [9], during the early stages of metal deposition, a linear relationship between the current density (I) and the function of deposition time $(t - t_0)^{1.5}$ corresponds to progressive nucleation and a three dimensional growth of the nuclei limited by a slow diffusion process. A linear relationship between the current density and $(t - t_0)^{0.5}$ corresponds to instantaneous nucleation followed by three-dimensional growth under diffusion control.

For the 600-grit polished stainless steel substrates, a linear relationship between current density and $(t - t_0)^{1.5}$ was observed (Fig. 10). Different results were obtained when the oxidizing temperature was lower. As shown in Figs 11 and 12, a linear relationship between the current density and $(t - t_0)^{0.5}$ was found for the electrodes furnace oxidized at 200 °C and 300 °C. For the as-received stainless steel substrates, the mechanism was similar to that for the low temperature oxidized surfaces (Fig. 13). All data were checked for the best fit before choosing the most appropriate model.

Instantaneous nucleation appeared to be the mechanism for the as-received and lower temperature oxidized stainless steel surfaces, but progressive nucleation occurred with the higher temperature furnace oxidized stainless steel cathodes, which is in agreement with the results of the SEM examination.

The analysis of the current density and $(t - t_0)^n$ relationship suggested that the lower temperature oxidation not only enhanced copper electrodeposition by reducing the overpotential, but the mechanism also changed from progressive to nearly instantaneous nucleation.

Essentially, the nucleation and growth behaviour of the copper electrodeposits on the various substrates is based on the respective charge-transfer rates and active sites initially available on the cathode surface. It is known that any films formed on the

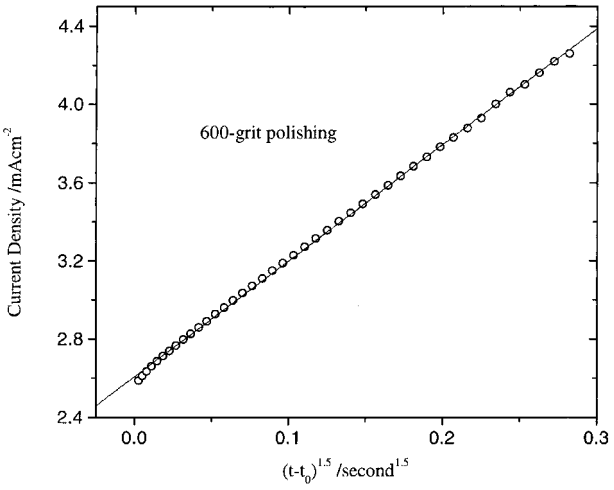

Fig. 10. Relationship between current density against $(t - t^0)^{1.5}$ for copper deposition on 600 grit polished stainless steel substrates from the copper sulfate electrolyte at −600 mV vs Hg/Hg_2SO_4.

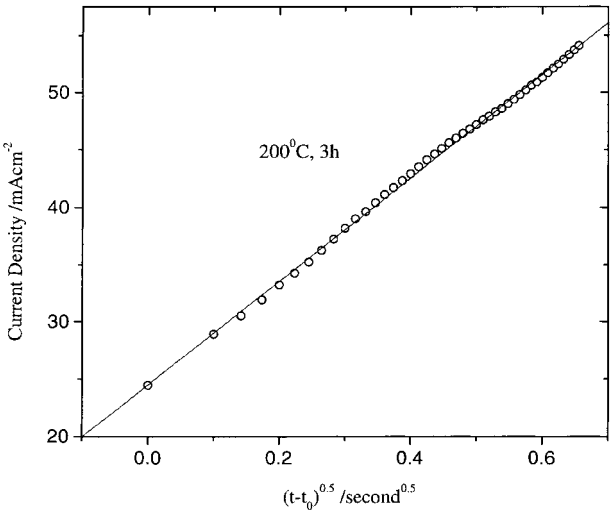

Fig. 11. Relationship between current density against $(t - t^0)^{0.5}$ for copper deposition on 200 °C furnace oxidized stainless steel substrates from the copper sulfate electrolyte at −600 mV vs Hg/Hg_2SO_4.

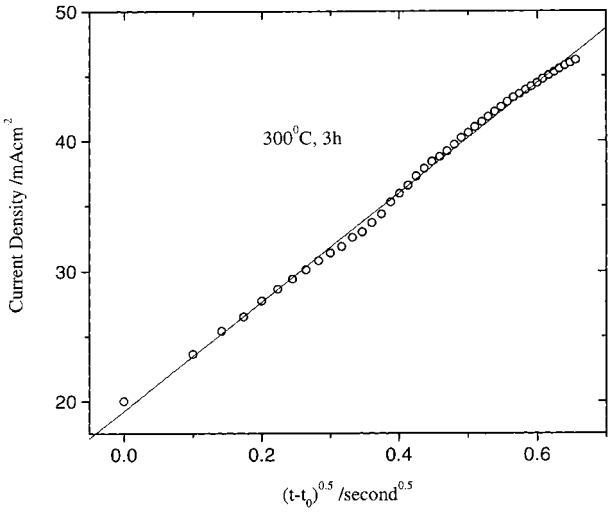

Fig. 12. Relationship between current density against $(t - t^0)^{0.5}$ for copper deposition on 300 °C furnace oxidized stainless steel substrates from the copper sulfate electrolyte at −600 mV vs Hg/Hg_2SO_4.

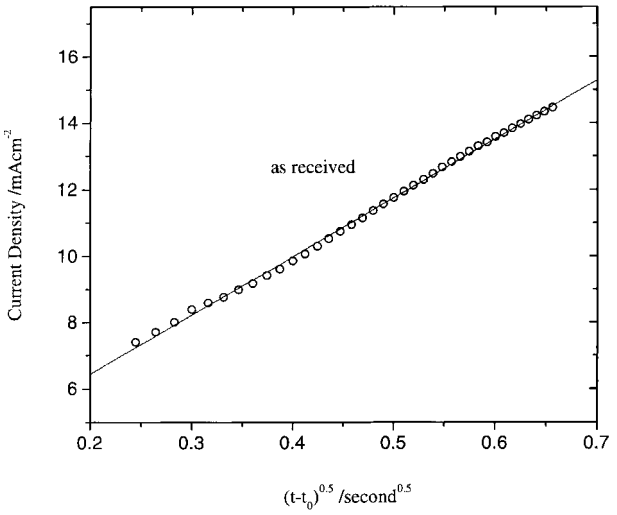

Fig. 13. Relationship between current density against $(t - t^0)^{0.5}$ for copper deposition on as-received stainless steel substrates from the copper sulfate electrolyte at −600 mV vs Hg/Hg_2SO_4.

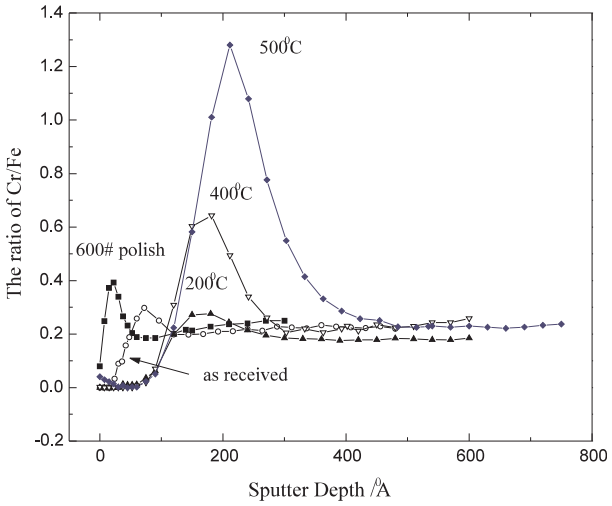

Fig. 14. Auger depth profile of Cr:Fe atomic ratio of 316 L stainless steel cathodes treated at different conditions for 3 h. Key: (–■–) 600 grit polish; (–○–) as-received; (–▲–) 200 °C; (–▽–) 400 °C; (–◆–) 500 °C.

electrodes can influence either of these factors. Different mechanisms have been proposed to describe the electron transfer reactions at metal electrodes covered by semiconducting or insulating films [11]. For thin films less than a few nanometres, the dominating electron transfer mechanism is elastic or inelastic tunneling. For thicker films, the electron transfer mainly depends on the semiconducting properties of the films. According to the Auger surface composition analysis (Table 1), the oxide films formed by furnace oxidation on the stainless steel should be treated as thicker films. Conductivity changes were considered to be one possible reason for the overpotential and current density changes observed. Measurements revealed that as the oxidation temperature increased, the oxide films became thicker and conductivity decreased to some degree as expected. However, the oxide films formed at lower temperature caused considerably more depolarization and enhanced copper growth than might be expected purely from a resistance standpoint. The possible exception is when the films become thicker and clearly more resistive, such as observed at 600 °C.

Liao *et al.* [12] studied the influence of different nitric acid passivation treatments for the 316 L stainless steel on the pitting corrosion resistance. The Cr : Fe atomic ratio depth profiles near the surface of specimens resulting from various surface treatments were found to influence the extent of the pitting corrosion resistance. It was felt that the ratio of Cr : Fe would offer a possible explanation for the overpotential and current density changes observed in this research. Unfortunately, no reports of changes in electrochemical behaviour with various ratios of Cr : Fe were found in the literature. Additional studies are planned in this area to attempt to clarify this issue.

The Cr : Fe atomic ratio depth profiles of the 316 L stainless steel with different surface treatments are given in Fig. 14. All curves show a peak value of the Cr : Fe ratio at various depths. For different specimens, the Cr : Fe ratio changed and the peak value was different. The peak Cr : Fe ratio increased and the location where it occurred moved inward toward the bulk specimen as the oxidation temperature treatment increased. For the substrate oxidized at 200 °C, the peak value was about 0.27 and occurred at a depth of 135 Å. The peak value increased to 0.64 at a depth of 180 Å as the oxidized temperature increased to 400 °C. For the substrate oxidized at 500 °C, the peak value was further increased to 1.28 at a depth of 210 Å. For as-received stainless steel substrates, the peak value was 0.30 and was located at a depth of 72 Å. After 600-grit mechanical polishing, the peak value increased to 0.39 and the location moved toward the surface of specimen located at a depth of only 25 Å. Based on these results, it seems that lower peak values give enhanced nucleation and growth of the copper. Therefore, the Cr : Fe atomic ratio near the electrode surface may influence the electrochemical properties of the oxide films. The reproducibility is good for the substrates oxidized at low temperature, similar results being obtained for repeated use. For substrates oxidized at high temperature, the cathode colour became lighter with use but the deposits were not extensively evaluated. Further studies are necessary to confirm these possible mechanisms and their effects on electrochemical activity, however, the results clearly illustrate that the Cr : Fe ratio is one factor influencing the initial nucleation and growth of copper.

4. Conclusions

Furnace oxidation of stainless steel at temperatures from 200 to 600 °C produced different thin surface oxide films which appeared to have a major effect on copper nucleation. The colour, thickness and relative composition of the stainless steel films changed with oxidation temperature. As the treatment temperature

increased from 200 to 600 °C, the colour of the stainless steel oxide films changed from light yellow to gold and finally blue. The thickness of the oxide films increased from 240 to 540 Å and the resistance increased from about 1.0×10^{-2} to $2.6\times10^{-2}\,\Omega$ with increasing temperature.

The effects of the oxidation of stainless steel cathodes on copper nucleation can be divided into two categories, separated by a transition temperature of approximately 400 °C. Above the transition temperature, the oxide layer acts a blocking film, providing a barrier to electron transfer causing copper nucleation to be progressive and giving low surface coverage for 1.5 s at a potential of −600 mV. Below the transition temperatures (200 °C and 300 °C), enhanced nucleation, lower required overpotential and higher observed current density were obtained. Nucleation appeared to be instantaneous with a very fine crystallite size giving high coverage of the surface in 0.5 s at a potential of −600 mV. This behaviour may be related to the high conductivity, low Cr : Fe ratio peak value near the surface or other factors such as microroughening or changes in the defect structure.

Compared to the 600-grit mechanical polishing substrate, the copper nuclei were finer and denser than obtained on the as-received substrate.

Based on the theory developed by Thirsk and Harrison, progressive nucleation with three-dimensional growth under a diffusion controlled mechanism was observed for the 600-grit polishing substrate and substrates treated at 500 °C and 600 °C. For the as-received substrate and substrates treated at lower temperature, the copper nucleation mechanism appeared to be instantaneous but was also diffusion controlled.

The results obtained in this study suggest that copper nucleation can be strongly modified by thermal oxidation of stainless steel in much the same way as previously reported for oxidized and plasma treated titanium [8, 9]. Results were reproducible and the trends established were consistent with other reported studies. Additional research is necessary to further elucidate the causes of this behaviour and to identify other processing aspects which could influence the surface activity and nucleation of electrodeposited copper. Although the results are probably less important for thick deposits, the differences noted could be significant in producing foil or starter sheets when a stainless steel blank is used.

References

[1] J. L. Delplancke, M. Sun, T. J. O'Keefe and R. Winand, *Hydrometall.* **23** (1989) 47.
[2] *Idem, ibid.* **24** (1990) 179.
[3] H. Sun, J. L. Delplancke, R. Winand and T. J. O'Keefe, 'Copper 91–Cobalt 91', Vol. 3 (1991) 405.
[4] G. M. Rao and W. C. Cooper, *Hydrometall.* **4** (1979) 185.
[5] K. S. Fraser and W.C. Cooper, *Surf. Technol.* **8** (1979) 385.
[6] J. B. D. Cusminsky, *J. Crystal Growth*, **41** (1977) 330.
[7] Jian Zhang, PhD dissertation, University of Missouri-Rolla, Rolla, MO (1994).
[8] Kuo-shi Teng, PhD dissertation, University of Missouri-Rolla, Rolla, MO (1995).
[9] H. R. Thirsk and J. A. Harrison, 'A Guide to the Study of Electrode Kinetics', Academic Press, New York (1972), p. 115.
[10] T. Fukuzuka, K. Shimogori, H. Satoh and F. Kamikubo, Titanium'80 Science and Technology, Proceedings of the Fourth International Conference on Titanium, Vol. 4 (1980) 2782.
[11] R. R. Dogonadze, A. M. Kuznetsov and J. Zak, *Electrochim. Acta* **22** (1977) 967.
[12] Hsien-tsung Liao, MS thesis, University of Missouri-Rolla, Rolla, MO (1993).